Thin Solid Films xxx (2009) xxx–xxx

Contents lists available at ScienceDirect

Thin Solid Films

journal homepage: www.elsevier.com/locate/tsf

The effect of composition on the bond structure and refractive index of silicon nitride deposited by HWCVD and PECVD

V. Verlaan [a], A.D. Verkerk [a], W.M. Arnoldbik [a], C.H.M. van der Werf [a], R. Bakker [a], Z.S. Houweling [a], I.G. Romijn [b], D.M. Borsa [b], A.W. Weeber [b], S.L. Luxembourg [c], M. Zeman [c], H.F.W. Dekkers [d], R.E.I. Schropp [a,*]

[a] Utrecht University, Faculty of Science, Debye Institute for Nanomaterials Science, Nanophotonics — Physics of Devices, P.O. Box 80.000, 3508 TA Utrecht, The Netherlands
[b] ECN Solar Energy, Petten, The Netherlands
[c] DIMES, Delft University of Technology, The Netherlands
[d] IMEC, Leuven, Belgium

A R T I C L E I N F O

Available online xxxx

Keywords:
Hot Wire CVD
Silicon nitride

A B S T R A C T

Silicon nitride (SiN_x) is a material with many applications and can be deposited with various deposition techniques. Series of SiN_x films were deposited with HWCVD, RF PECVD, MW PECVD and LF PECVD. The atomic densities are quantified using RBS and ERD. The influence of the atomic densities on the Si–N and Si–Si bond structure is studied. The density of N–N bonds is found to be negligible. New Si–N FTIR proportionality factors are determined which increase with increasing N/Si ratio from $1.2\cdot10^{19}$ cm^{-1} for Si rich films (N/Si=0.2) to $2.4\cdot10^{19}$ cm^{-1} for N rich films (N/Si=1.5). The peak position of the Si–H stretching mode in the FTIR spectrum is discussed using the *chemical induction model*. It is shown that especially for Si-rich films the hydrogen content affects the Si–H peak position. The influence of the composition on the refractive index of the films is discussed on the basis of the *Lorentz–Lorenz* equation and the *Kramers–Kronig* relation. The decreasing refractive index with increasing N/Si ratio is primarily caused by an increase of the band gap.
© 2009 Elsevier B.V. All rights reserved.

1. Introduction

Silicon nitride (SiN_x) has many applications and can be deposited using various chemical vapor deposition (CVD) techniques. To optimize the films for different applications, knowledge about the influence of the composition on the bonding structure and refractive index is necessary. To obtain this insight, the correlation between composition, bond structure and refractive index of SiN_x films deposited using different techniques is compared. By comparing these films, fundamental relations between the properties are obtained.

2. Experimental details

SiN_x films were deposited using Hot Wire (HW) CVD [1], radio frequency (RF) plasma enhanced (PE) CVD [2], pulsed low frequency (LF) PECVD [3] and microwave (MW) PECVD [4]. The composition of the films was varied by adjusting the silane to ammonia flow ratio, except for the LF PECVD films where only the substrate temperature was altered. The substrate temperatures during deposition were 450 °C for the HWCVD, 350 °C for MW PECVD, 235 °C for RF PECVD and between 200 and 500 °C for LF PECVD.

All films were subsequently analyzed with Fourier transform infrared spectroscopy (FTIR), Rutherford backscattering (RBS) and elastic recoil detection (ERD). The FTIR spectra were obtained under N_2 purging and afterwards corrected for coherent and incoherent reflections [5]. For an accurate determination of the ratio between the Si, N and H atoms, ERD [6] was applied employing a 50 MeV Cu^{8+} ion beam. Here a gas filled ionization chamber was used for background free detection for the separate elements. 2 MeV He^{+} ions were used for the RBS [7] measurements. The areal densities were determined by simulation of the RBS spectra with the ERD results as input for the RUMP simulation package [8]. The refractive indices and thicknesses were determined with either ellipsometry or reflection/transmission measurements.

3. Compositional properties

Fig. 1 shows the H, N and Si volume densities (in at/cm^3) as a function of the N/Si ratio. HWCVD and MW PECVD show similar trends. It is of interest that the Si density for HWCVD and MW PECVD films is almost invariable. For N rich (N/Si > 1.3) HWCVD films both the N and Si densities decrease. The H density is roughly constant for HWCVD and MW PECVD films with N/Si ratios larger than 0.5 and

* Corresponding author.
E-mail address: r.e.i.schropp@uu.nl (R.E.I. Schropp).

0040-6090/$ – see front matter © 2009 Elsevier B.V. All rights reserved.
doi:10.1016/j.tsf.2009.01.065

ARTICLE IN PRESS

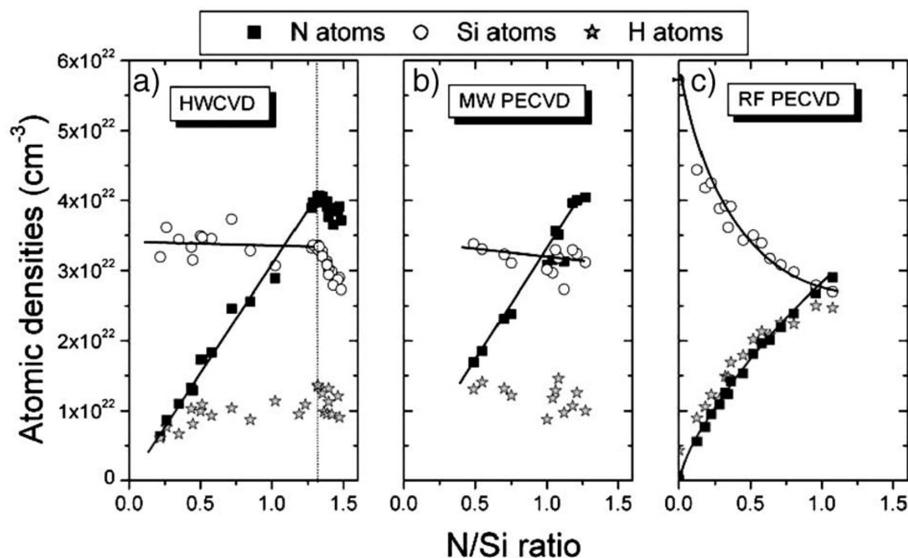

Fig. 1. The N, Si and H atomic densities for as-deposited (a) HWCVD, (b) MW PECVD, and (c) LF PECVD SiN_x films. The curves are added as a guide to the eye.

amounts to about $1 \cdot 10^{22}$ at/cm^3. The densities of the RF PECVD films show different trends; both the N and H densities increase for increasing N/Si ratios and the Si density decreases. These trends are possibly influenced by the deposition parameters and therefore they are not necessarily typical for the deposition technique used. The wide range of obtained compositions provides fundamental insight in the correlations between the composition, the bond structure and the refractive index.

4. Si–N and Si–Si bond structure

A frequently used technique to study the bond structure is FTIR. The largest peak in the FTIR spectra is found around 840 cm^{-1}, which is dominated by the Si–N stretching mode. A maximum for the integrated absorption [9] of the Si–N peak (I_{Si-N}) is reached at the N/Si ratio where the N density peaks (N/Si = 4/3).

The Si–Si and N–N bond densities are estimated by combining ERD, RBS and FTIR analysis. Eqs. (1) and (2) hold, under the assumption that the amounts of N and Si dangling bonds are negligible.

$$3N_N = [\text{Si–N}] + [\text{N–H}] + 2[\text{N–N}] \quad (1)$$

$$4N_{Si} = [\text{Si–N}] + [\text{Si–H}] + 2[\text{Si–Si}] \quad (2)$$

where N_N and N_{Si} are the atom densities and [X–Y] the density of bonds between atoms X and Y. The asymmetric bond densities are obtained from FTIR analysis, using the FTIR proportionality factors from Lanford and Rand [10] for N–H and Si–H and Bustarret et al. [11] for Si–N. The determined N–N and Si–Si densities are shown in Fig. 2 (a). Both bond densities show a similar trend for all samples. The density of Si–Si bonds is zero for N-rich films and increases with decreasing N/Si ratio. The density of N–N bond is negligible for all compositions. A Raman measurement of a HWCVD $SiN_{0.9}$ film

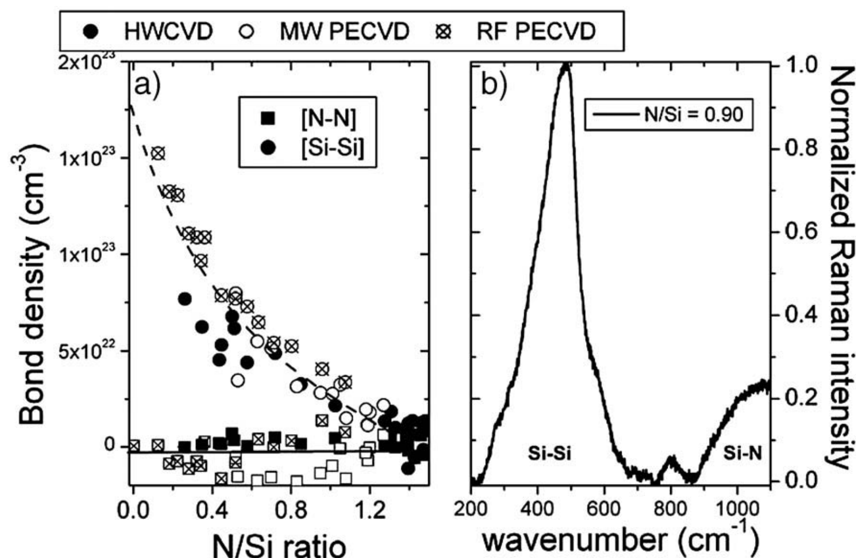

Fig. 2. (a) The calculated Si–Si and N–N bonds in SiN_x films deposited with different deposition techniques. The curves are added as a guide to the eye. (b) Raman spectrum of a $SiN_{0.9}$ film. The Si–Si contribution is clearly visible.

ARTICLE IN PRESS

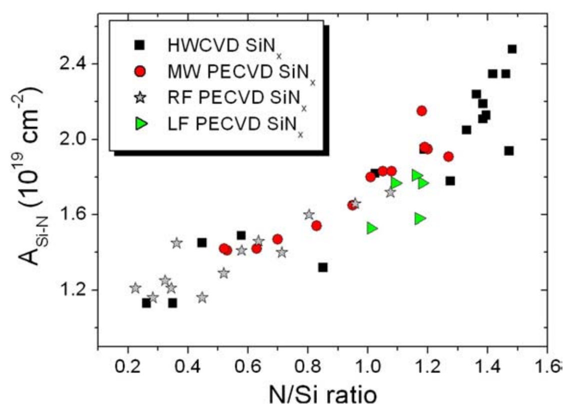

Fig. 3. The Si–N proportionality factor for films deposited with different techniques versus the N/Si ratio.

(Fig. 2(b)) confirms the presence of Si–Si bonds by the band that is present at 480 cm^{-1}.

Since the amount of N–N is negligible and the density of Si–N bonds can be calculated by multiplying I_{Si-N} with the FTIR proportionality factor A_{Si-N}, A_{Si-N} can be determined by rewriting Eq. (1) to:

$$A_{Si\text{-}N} = \frac{3N_N - [N\text{-}H]}{I_{Si\text{-}N}}. \quad (3)$$

This induces an error since the N–H proportionality factor changes with composition [12]. However, since $N_N \gg$ [N–H] the error caused by incorrect [N–H] in A_{Si-N} is limited to less than 2%. Fig. 3 shows A_{Si-N} for films in a wide range of N/Si ratios. A general increasing trend is present for all deposition techniques used. For Si-rich films the A_{Si-N} is $1.2 \cdot 10^{19}$ cm^{-2}. The value increases with increasing N/Si ratio to $2.4 \cdot 10^{19}$ cm^{-2} for N-rich films. A similar trend has been reported earlier, although they reported slightly smaller values between $0.8 \cdot 10^{19}$ and $2.0 \cdot 10^{19}$ cm^{-2} [11].

5. The position of the FTIR Si-H stretching mode

Fig. 4 shows the Si–H peak position for the present SiN_x films along with data found in literature [13–17]. For films with an N/Si ratio larger than 0.6, the Si–H peak positions are similar, for films with an N/Si ratio smaller than 0.6 discrepancies appear. These differences can be as large as 50 cm^{-1} for films with equal N/Si ratio. To obtain insight in the Si–H peak position in Si alloys, the *chemical induction method* [18–20] is applied. This model accounts for differences in the effective electronegativity sum that forms the local environment of the Si–H bonds and thus accounts for differences in primary, secondary and higher orders of back bonding. The Si–H peak position as a result of the back bonding configuration is described by:

$$\omega(\mathrm{cm}^{-1}) = 1630 + 49 \sum_{j=1}^{3} \chi_{A_j} \quad (4)$$

where χ_{Aj} is the effective electronegativity of the jth neighbor of the Si–H bond. The χ_{Aj} for each type of neighboring atom is determined as the geometric average by;

$$\chi_{A_j} = \left[\chi_j \chi_m^k\right]^{\frac{1}{(1+k)}} \quad (5)$$

where χ_j is the stability ratio of the electronegativity of each element (χ_{Si}=2.62, χ_N=4.49 and χ_H=3.55 [18]) and k is the number of second nearest sites (2 for N and 3 for Si). χ_m is the average electronegativity and thus accounts for the matrix effects. χ_m can consequently be determined using:

$$\chi_m = \left[\chi_{Si} \chi_N^r \chi_H^q\right]^{\frac{1}{(1+r+q)}} \quad (6)$$

where r is the N/Si ratio and q the H/Si ratio. Since χ_m changes by differences in N/Si and H/Si ratio, the Si–H peak position depends not only on the primary back bonding but also on the hydrogen content [20]. Because the hydrogen concentration can reach values as high as 30 at.%, this model should also account for $-Si-H_2$ and $-Si-H_3$ groups since they are likely to be present. This extends the model as reported so far. Each of the three back bonding possibilities for the Si host atoms is thus described by;

$$\chi_A^{Si} = \left[\chi_{Si} \chi_m^3\right]^{1/4} \quad (7)$$

$$\chi_A^{N} = \left[\chi_{N} \chi_m^2\right]^{1/3} \quad (8)$$

$$\chi_A^{H} = \left[\chi_{H}\right] \quad (9)$$

Eq. (6) shows that the Si–H peak position of each back bonding configuration is affected by the N/Si and H/Si ratios. The influence of the H/Si ratio in the layer is very small for near stoichiometric films, but it causes significant peak shifts for Si-rich films [20].

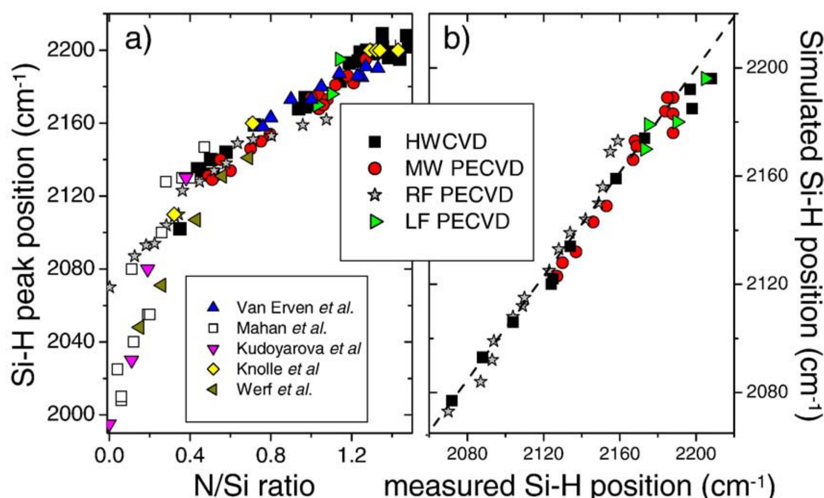

Fig. 4. (a) The Si–H peak position for a wide range of N/Si ratios for films deposited with different techniques. (b) The simulated versus the measured Si–H peak position. The dashed line represents prefect agreement between the two.

Please cite this article as: V. Verlaan, et al., Thin Solid Films (2009), doi:10.1016/j.tsf.2009.01.065

ARTICLE IN PRESS

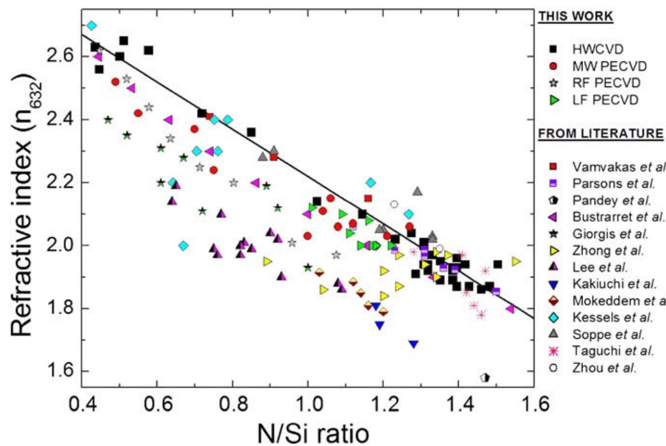

Fig. 5. Correlation between the refractive index at 632 nm and the N/Si ratio for SiN_x films deposited with different deposition techniques. The black line is a linear fit through the data of the HWCVD films.

To simulate the peak position of the Si–H stretching mode in the FTIR spectrum, the positions of all possible bond configurations are determined (using Eq. (4)) and scaled in intensity with their respective probabilities of occurrence. To determine these probabilities, a random bonding configuration and homogeneous atom distribution are assumed. By adding Gaussian shaped contributions (with a width of 90 cm^{-1}) for each back bonding configuration in proportion to their probability of occurrence of each back bonding configuration, the position of the combined Si–H stretching mode is simulated [18,19]. Fig. 4b shows the data for the simulated versus the measured peak positions. The close correlation shows that this model is appropriate and thus the influence of the hydrogen concentration on the position of the Si–H stretching mode peak.

6. Refractive index

Fig. 5 shows the refractive index at 632 nm, n_{632}, of the present films versus the N/Si ratio, combined with data from literature [11,21–29]. The understanding of the influence of the composition on the refractive index can be improved by using the *Lorentz–Lorenz* formula. This equation relates the total polarizability of a specific medium consisting of perfect spheres to its refractive index by

$$\frac{n^2-1}{n^2+2} = \frac{4\pi}{3}\sum_k N_k\alpha_k, \qquad (10)$$

in which n is the refractive index, α_k is the electronic polarizability and N_k is the atomic density of atom k. Eq. (10) shows that films with equal N/Si ratio but smaller mass density have smaller values for n_{632}. So the dissimilarity in n_{632} for films with equal N/Si ratio might be caused by differences in mass density. Consequently, the refractive index alone is not a suitable way to determine the N/Si ratio in SiN_x films.

Since the *Lorentz–Lorenz* equation predicts an increase of n_{632} when more N atoms are incorporated (as is the case for the HWCVD and MW PECVD SiN_x films), these equation fails to explain the observed negative trend with increasing N/Si ratio.

The correct explanation for the wide spread in refractive index may be found in the increase of the band gap energy with increasing N/Si ratio. According to the *Kramers–Kronig* dispersion relation the refractive index is affected by the blue shift of the absorption. If the refractive index is probed in a region of strong dispersion, the blue shift consequently causes a decrease of n. Since the band gap is the largest for the N-rich films, the refractive index is lowest for these samples. To confirm this hypothesis numerical simulations of the *Kramers–Kronig* relation are performed and show good agreement with the experimental data [30].

7. Conclusions

The atomic volume densities of HWCVD, RF PECVD, MW PECVD and LF PECVD silicon nitride samples are quantified using ERD and RBS. For HWCVD and MW PECVD the Si and H volume density is equal for all compositions. These atomic densities are used to determine their influence on the Si–N, N–N and Si–Si bond structure. The amount of N–N bonds is found to be negligible for all samples, and the amount of Si–Si bonds decreases with increasing N/Si ratio.

New Si–N FTIR proportionality factors were calculated, which increase with increasing N/Si ratio from $1.2\cdot10^{19}$ cm^{-1} for Si-rich films (N/Si=0.2) to $2.4\cdot10^{19}$ cm^{-1} for N rich films (N/Si=1.5). The peak position of the Si–H stretching mode in the FTIR spectrum is discussed using the *chemical induction model*. This shows that the N/Si ratio is not solely dependent on the N/Si ratio but also on the hydrogen concentration. The influence of the composition on the refractive index of the films is discussed with the *Lorentz–Lorenz* equation and the *Kramers–Kronig* relation. No general correlation between the N/Si ratio and the refractive index is present. The *Lorenz–Lorentz* equation fails to describe the influence of the composition on the refractive index. The decreasing refractive index with increasing N/Si ratio is likely to be caused by an increase of the band gap.

Acknowledgement

Dr. E.E.H. van Faassen is acknowledged for fruitful discussions.

References

[1] V. Verlaan, Z.S. Houweling, C.H.M. Van der Werf, I.G. Romijn, A.W. Weeber, H.D. Goldbach, R.E.I. Schropp, Thin Solid Films 516 (2008) 533.
[2] S.L. Luxembourg, F.D. Tichelaar, P. Kus, M. Zeman, Mater. Res. Soc. Proc. 1066 (2008) A07-04.
[3] H.F.W. Dekkers, S. de Wolf, G. Agostinelli, F. Duerinckx, G. Beaucarne, Sol. Energy Mater. Sol. Cells 90 (2006) 3244.
[4] I.G. Romijn, W.J. Soppe, H.C. Rieffe, W.C. Sinke, and A.W. Weeber. Proc. 15th workshop on Crystal. Si solar cells and modules.
[5] N. Maley, Phys. Rev., B 46 (1992) 2078.
[6] W.M. Arnold Bik, F.H.P.M. Habraken, Rep. Prog. Phys. 56 (1993) 2530.
[7] W.K. Chu, J.W. Mayer, M.A. Nicolet, Backscattering Spectroscopy, Academic Press, NY, 1978.
[8] L.R. Doolittle, Nucl. Instrum. Methods B9 (1985) 344.
[9] M. Cardona, Phys. Status Solidi B 118 (1983) 463.
[10] W.A. Lanford, M.J. Rand, J. Appl. Phys. 49 (1978) 2473.
[11] E. Bustarret, M. Bensouda, M. Habrard, J. Breyere, S. Poulin, S. Gujrathi, Phys. Rev., B 38 (1998) 8171.
[12] V. Verlaan, C.H.M. van der Werf, W.M. Arnoldbik, H.D. Goldbach, R.E.I. Schropp, Phys. Rev., B 73 (2006) 195333.
[13] A.J.M. van Erven, R. Bosch, O. Voigth, S. Petri, M.D. Blijker, Proc. Photovoltaic Solar Energy Conference, 2004.
[14] W.R. Knolle, J.S. Ossenbach, J. Appl. Phys. 58 (1985) 1248.
[15] V.K. Kudoyarova, A.A. Aivazov, B.G. Budaguan, I.V. Filatova, Mater. Res. Soc. Symp. Proc. 284 (1993) 127.
[16] A.H. Mahan, A.C. Dillon, I.M. Gedvillas, D.L. Williamson, J.D. Perrin, J. Appl. Phys. 94 (2003) 2360.
[17] C.H.M. van der Werf, H.D. Goldbach, J. Loffler, A. Scarfo, A. Kylner, B. Stannowski, W. Arnoldbik, A. Weeber, H. Rieffe, W. Soppe, R.E.I. Schropp, Thin Solid Films 501 (2006) 51.
[18] G. Lucovsky, Solid State Commun. 29 (1979) 517.
[19] G.N. Parsons, G. Lucovsky, Phys. Rev., B 41 (1990) 1664.
[20] A.A. Aivazov, B.G. Budaguan, D.A. Stryahiliv, J. Non-Cryst. Solids 167 (1994) 185.
[21] F. Giorgis, F. Giuliani, C. Pirri, E. Tresso, C. Summonte, R. Rizzoli, R. Galloni, A. Desalvo, P. Rava, Philos. Mag., B 77 (1998) 925.
[22] H. Kakiuchi, Y. Nakahama, H. Ohmi, K. Yasutake, K. Yoshi, Y. Mori, Thin Solid Films 479 (2005) 17.
[23] W.M.M. Kessels, J. Hong, F. Assche, J. Moschner, T. Lauinger, W.J. Soppe, A.W. Weeber, A. Schram, M.C.M. van der Sanden, J. Vac. Sci. Technol., A 20 (2002) 1704.
[24] J. Lee, R. Ryoo, M.S. Jhon, K. Cho, J. Phys. Chem. Solids 56 (1995) 293.
[25] K. Mokeddem, M. Aoucher, T. Smail, Superlattices Microstruct. 40 (2006) 598.
[26] R.K. Pandey, L.S. Patil, J.P. Bange, D.K. Gautam, Opt. Mater. 27 (2004) 139.
[27] W.J. Soppe, J. Hong, W. Kessels, M. van der Sanden, W.M. Arnoldbik, C. Devilee, S. Schiermeier, A.W. Weeber, Proc. IEEE PVSEC (2002) 158.
[28] K. Taguchi, M. Yoshimoto, J. Saraie, A. Chayahara, Y. Horino, Jpn. J. Appl. Phys. 43 (2004) L1403.
[29] K. Zhu, K. Elgaid, C. Wolkinson, I. Thayne, Jpn. J. Appl. Phys. 45 (2006) 8388.
[30] V. Verlaan. Silicon nitride at high growth rate using hot wire chemical vapor deposition. PhD-thesis 2008. ISBN: 978-90-393-4882-6.

Please cite this article as: V. Verlaan, et al., Thin Solid Films (2009), doi:10.1016/j.tsf.2009.01.065